Journal of Thermal Analysis and Calorimetry, Vol. 88 (2007) 1, 71–76

THERMAL BEHAVIOUR OF CuS (COVELLITE) OBTAINED FROM COPPER–THIOSULFATE SYSTEM

Claudia Maria Simonescu[1*], *V. S. Teodorescu*[2], *Oana Carp*[3], *Luminita Patron*[3] *and Camelia Capatina*[4]

[1]Department of Inorganic Technology and Environmental Protection, Faculty of Applied Chemistry and Materials Science, University 'Politehnica' of Bucharest, Polizu Street, No. 1–7, 011061, Bucharest, Romania
[2]National Institute for Material Physics, P.O.Box. Mg-7, Bucharest-Magurele, 77125, Romania
[3]Institute of Physical and Chemical 'Ilie Murgulescu', Splaiul Independentei Street, No.202, Bucharest, Romania
[4]Department of Environmental Engineering, University 'Constantin Brancusi', Genova Street, No. 3, 210152, Targu-Jiu, Romania

Thermal behaviour of CuS (covellite) obtained from the $Cu(CH_3COO)_2 \cdot H_2O$ and $Na_2S_2O_3 \cdot 5H_2O$ system, working at different molar ratio (1:6 and 1:4) in presence/absence of NH_4VO_3, was studied. It was established that the presence of vanadium in the system induces a densification of CuS nodules, but do not change the hexagonal CuS structure. It has an important influence in thermal behaviour of copper sulfide CuS obtained also. The morphological characteristics of CuS play an important role in the thermal stability and the stoichiometry of the thermal decompositions.

Also, the possibility to obtain copper sulfides with greater cooper content was investigated.

Keywords: *copper sulfide, thermal oxidation*

Introduction

Transition metal chalcogenides have attracted considerable attention in recent decades due to their interesting optical and electrical properties [1–5]. Since the historic discovery of the photovoltaic properties of Cu_xS thin films in contact with CdS films [6], the copper-sulfur systems have received particular attention related to the achievement of solar cells [7, 8], solar control and solar absorber coatings [9–11]. On the other hand, because of great importance in copper pyrometallurgy, oxidation processes of different copper sulfides were subjected of considerable interest [12–18].

As a promising method for the preparation nanocrystallites of sulphides, the decomposition of complex precursors containing metal sulfur (either in solution or solid state) would be regarded as an efficient synthetic route [19–21].

It was extensively studied the thermal behaviour of natural and synthesized copper sulfides [12–15, 22–34]. It was established that the CuS thermal decomposition is a multistep process, and depending on experimental conditions (temperature, atmosphere) different copper sulfides ($Cu_{1.8}S$ and/or Cu_2S), oxides (Cu_2O and CuO), sulfates (Cu_2SO_4, $CuSO_4$), oxysulfates ($CuO \cdot CuSO_4$) were formed [24–32]. Generally, the final product obtained from CuS thermal decomposition is Cu_2O, but in case of mechanochemically synthesized nanocrystalline CuS particles thermal decomposition is obtained Cu instead of Cu_2O, which is stable up to 1100°C [23].

In this article, is presented the influence of different morphological characteristics of the prepared CuS on their thermal behaviour as expressed by thermal stability and decomposition stoichiometry.

Experimental

Materials

As raw materials in CuS synthesis copper acetate, ammonium metavanadate and, sodium thiosulfate of reagent quality were used (Merck Chemistry Co. Ltd.).

Reactions were conducted at the medium pH (5,5) at different Cu^{2+}:$S_2O_3^{2-}$ molar ratios, 1:6 and respective 1:4, in the presence or absence of NH_4VO_3. One of the CuS sample was obtained by system Cu^{2+}:V^{5+}:$S_2O_3^{2-}$ used in order to copper vanadium mixed sulfide obtained.

Sample 1

1.996 g (10 mmoles) $Cu(CH_3COO)_2 \cdot H_2O$, and 1.17 g (10 mmoles) NH_4VO_3 was mixed with 9.92 g (40 mmoles) $Na_2S_2O_3 \cdot 5H_2O$ in 200 mL distillated water. After continuous stirring for 10 min the solid compounds were dissolved and a yellow solution was obtained. The initial pH of the solution was 7. After 20 min of stirring, the yellow solution is changed into a brown-yellow solution (temperature about 45°C)

* Author for correspondence: clausimo2003@yahoo.co.uk

1388–6150/$20.00

Akadémiai Kiadó, Budapest, Hungary
Springer, Dordrecht, The Netherlands

which furthermore is converted in a brown solution and a green-brown precipitate (temperature about 70°C). After another 15 min of heating the temperature of solution was 92°C and the solution changed into a green solution. The colour of precipitate was green-black at this temperature. This mixture was maintained at 90±5°C temperature by continuously heating and stirring for two hours. At the end, this mixture was cooled at room temperature and the precipitate was filtered and washed with distilled water. The final product was dried at room temperature.

Sample 2

1.996 g (10 mmoles) $Cu(CH_3COO)_2 \cdot H_2O$ was mixed with 14.88 g (60 mmoles) $Na_2S_2O_3 \cdot 5H_2O$ in 200 mL distilled water. The same yellow solution was obtained after 5 min of stirring with heating (temperature about 60°C). The yellow solution obtained changed into a brown-yellow solution after 30 min of stirring at 70°C. After another 10 min brown-yellow was converted into a brown solution and a green-brown precipitate. When the temperature reached 92°C the brown solution changed into a green solution, and the green-brown precipitate changed into a green-black precipitate. This mixture was heated and stirred for two hours at 90±5°C, whereupon the black-violet solution and a black precipitate were formed. Then the solution with precipitate was cooled at room temperature. After filtering and washing with distilled water, the final product was dried at room temperature.

Sample 3

1.996 g (10 mmoles) $Cu(CH_3COO)_2 \cdot H_2O$ was mixed with 9.92 g (40 mmoles) $Na_2S_2O_3 \cdot 5H_2O$ in 200 mL distilled water. After 10 min of stirring with heating a yellow solution was obtained. The colour of the solution changed in brown-yellow after 35 min of stirring with heating (temperature about 50°C). After other 20 min of heating with stirring the brown-yellow solution was changed into a brown solution, and precipitate changed into a green-brown precipitate. Temperature at this point was 71°C. The green-black precipitate was obtained after other 20 min of heating when temperature got 92°C. A black precipitate was obtained after 1 h of stirring at 90±5°C. The solution with precipitate was cooled at room temperature. After filtering and washing with distilled water, the final product was dried at room temperature.

Methods

The samples obtained from these three systems were characterized by IR Spectroscopy, X-ray powder diffraction (XRD), transmission electron microscopy (TEM), and selected area electron diffraction (SAED). The elemental chemical analyses were performed by an Electronics SPD 1200A ICP emission analyzer with a pump flow of 1.85 mL min^{-1} and a flow rate of the auxiliary gas (Ar 99.99%) of 0.5 L min^{-1}. The IR spectra were recorded on a FTIR 620 (Jasco, Japan) spectrophotometer in the 400-4000 cm^{-1} range using KBr pellets. Powder X-ray diffraction (XRD) was used to characterize the sample. Data were collected on the Shimadzu XRD6000 and Philips Xpert X-ray diffraction-diffractometers. Transmission electron microscopy (TEM) was applied to determine the morphology of the prepared products by a specific methods for crystalline powders study. These powders were dispersed in alcohol and then they were deposited on a TEM grid with carbon support. Selected area electron diffraction (SAED) patterns were obtained from polycrystalline particles aggregates. TEM study was performed using a Jeol 200CX electron microscope. Thermal measurements were performed on a Q-1500 Paulik–Paulik–Erdey derivatograph, at heating rates of 2.5–5 K min^{-1} and with sample mass of ~20 mg.

Results and discussion

Characterization of the sulfides

The elemental chemical analysis of the powders obtained from these systems at 90±5°C showed that all the powders are copper monosulfide. Two of them were hydratated with 1 and 0.7 H_2O molecules. This result was confirmed by IR spectrum which showed that there are no impurities, e.g., thiosulfate, acetate, vanadate, or other impurities, which could be detected in the samples. The band presents at 3400–3500 cm^{-1} (Fig. 9) is assigned water molecules. The copper sulfide CuS samples 1 and 2 present this band.

The XRD patterns of a copper monosulfide prepared are shown in Figs 1–3. All the copper mono-

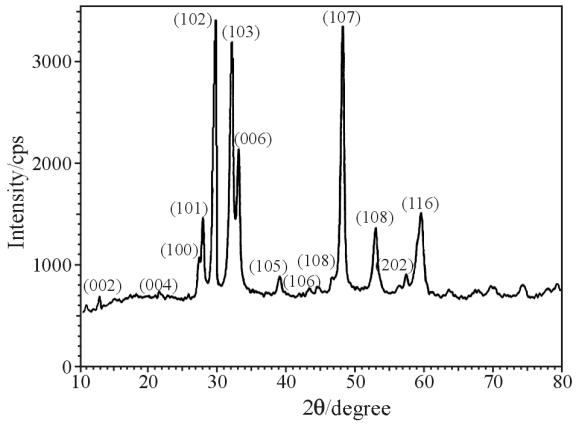

Fig. 1 XRD pattern of the copper monosulfide obtained from copper acetate, ammonium metavanadate and sodium thiosulfate system (1:1:6) at 90±5°C after 2 h

sulfide peaks in the pattern correspond to the reflections of hexagonal phases (ASTM File No. 6-0464 and ASTM File No. 78–877) and the pattern indicates that the prepared product is crystalline [35, 36].

The TEM investigation of the copper sulfide powder reveals the presence of polycrystalline aggregates of CuS hexagonal phase. Figure 4 shows such aggregates which are formed by nanometric CuS crystallites, obtained in the copper acetate, ammonium metavanadate and sodium thiosulfate (1:1:6) system. The morphology of these aggregates is nearly spherical and changes slowly depending of the composition of the system. The size of the CuS nanocrystallites is between 20 and 30 nm, as can be easy observed from the variation of the Bragg contrast in a polycrystalline aggregate. Figure 5 shows the SAED pattern corresponding to the sample exposed in Fig. 4. Only reflexions of the hexagonal CuS phase are present. The SAED patterns for all the analyzed samples are similar.

The CuS aggregates can be characterized as polycrystalline spherical nodules. The diameter of these nodules is between 200 and 300 nm. The spherical nodules obtained from system Cu^{2+}:$S_2O_3^{2-}$ (1:6) look to be less compact as the nodules obtained in the system with vanadium. By comparing Figs 4 and 6 is possible to conclude that the presence of vanadium in the system induce a densification of CuS nodules, but do not change the hexagonal CuS structure [37].

From system copper acetate and sodium thiosulfate at molar ratio (1:4), the spherical nodules are about 450 nm in average and the morphology of CuS nanocrystallites is radial, as can be seen in Fig. 7 [38]. In this case, the nodules can be the result of successive nucleation of CuS crystallites around a center.

Particle dimension was determined from TEM study, but also from XRD patterns using Scherrer formula [40]:

$$D=0.91\lambda/(\beta\cos\theta)$$

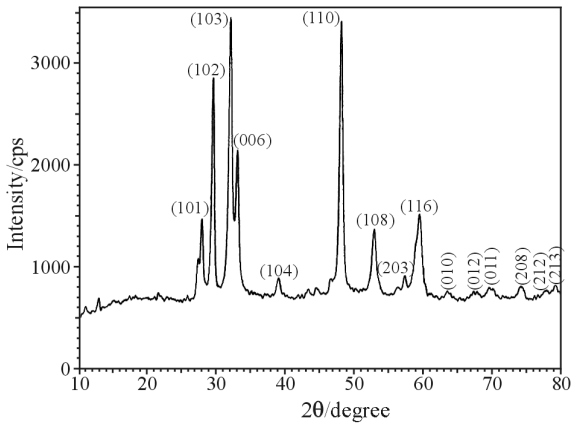

Fig. 2 XRD pattern of the copper monosulfide obtained from system copper acetate and sodium thiosulfate (1:6) at 90±5°C after 2 h

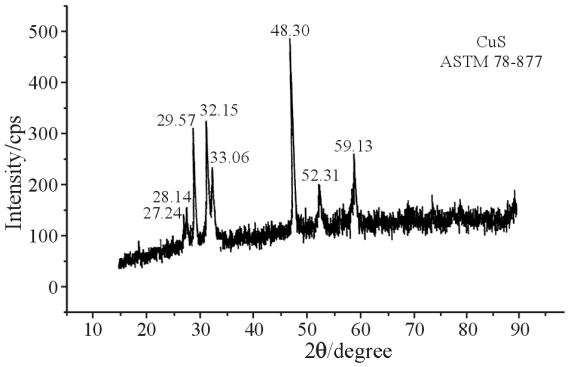

Fig. 3 XRD pattern of the copper monosulfide obtained from system copper acetate and sodium thiosulfate (1:4) at 90±5°C after 2 h

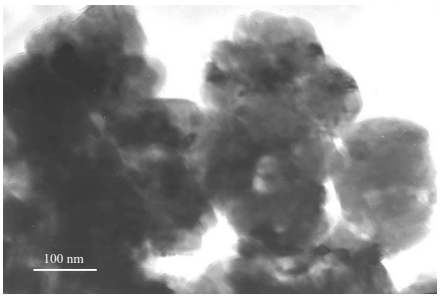

Fig. 4 Transmission electron microscopy of copper sulfide CuS from system copper acetate, ammonium metavanadate and sodium thiosulfate (1:1:6) at 90±5°C after 2 h

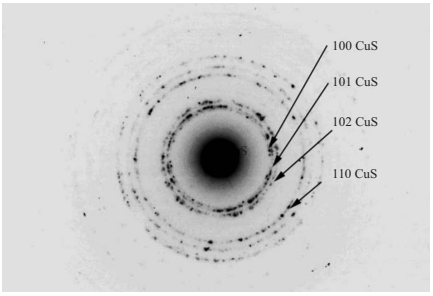

Fig. 5 SAED pattern obtained from aggregate of copper sulfide polycrystallites presented in Fig. 4

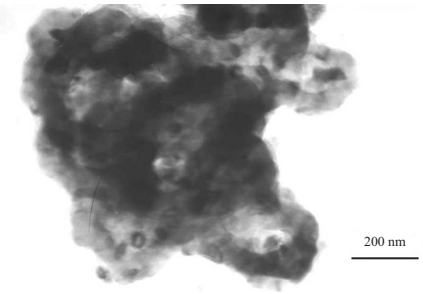

Fig. 6 Morphology of an aggregate of spherical nodules of copper monosulfide crystallites obtained from Cu^{2+}: $S_2O_3^{2-}$ (1:6) system

where: *D*=crystallite dimension, λ=wavelength (CuK_α), β=peak's half-width, θ= the diffraction angle of the peaks with relative intensity higher than 10.

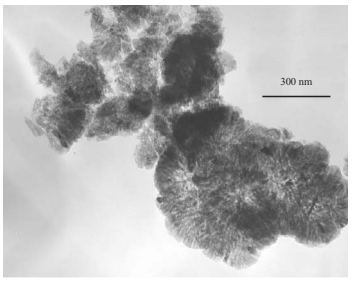

Fig. 7 Morphology of an aggregate of spherical nodules of copper monosulfide crystallites obtained from Cu^{2+}:$S_2O_3^{2-}$ (1:4) system

Thermal behaviour of the sulfides

The thermal decomposition curves (TG, DTG and DTA) of the three copper sulfides (CuS) are depicted in Figs 8, 10, 11.

Generally, the thermal oxidation of natural and precipitated covellite (CuS) studies mention the existence of four steps [21–28].

- formation of lower sulfur content sulfides ($Cu_{1.8}S$ and/or Cu_2S) associated with oxidation of the evolved sulfur to SO_2;
- oxidation of the existing sulfides either to copper oxides (Cu_2O and CuO, the late can be formed also by Cu_2O oxidation) or two copper sulfates (Cu_2SO_4, $CuSO_4$, the late is formed either by direct oxidation of Cu_2O, or reaction between liberated SO_2 and Cu_2O);
- oxysulfates formation ($CuSO_4$, and $CuO{\cdot}CuSO_4$) by reaction between copper oxide, oxygen and liberated SO_2;
- decomposition of oxysulfates with CuO formation.

The thermal decomposition of $CuS{\cdot}H_2O$ obtained from Cu^{2+}:V^{5+}:$S_2O_3^{2-}$ (1:1:6) system starts with

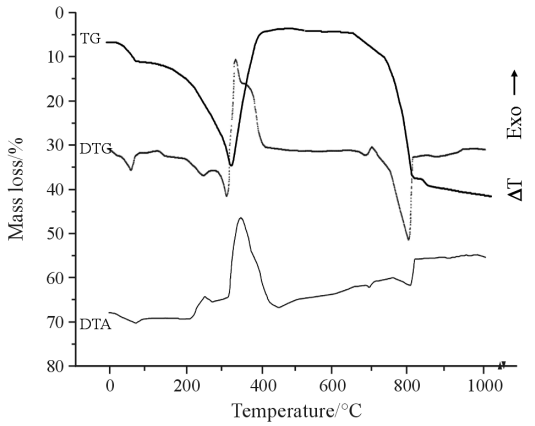

Fig. 8 TG, DTG and DTA curves of $CuS{\cdot}H_2O$ obtained from Cu^{2+}:V^{5+}:$S_2O_3^{2-}$ (1:1:6) system

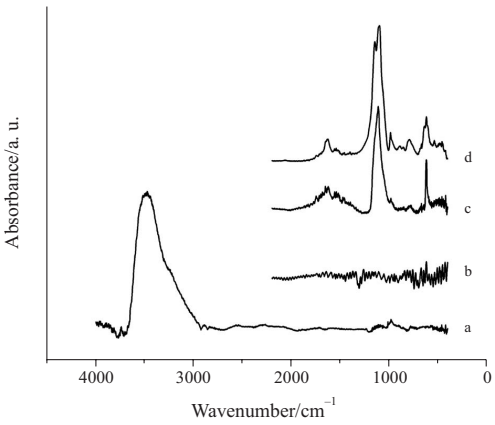

Fig. 9 IR spectra of $CuS{\cdot}H_2O$ obtained from Cu^{2+}:V^{5+}:$S_2O_3^{2-}$ (1:1:6) system and its decomposition products: a – $CuS{\cdot}H_2O$; b – $Cu_{1.8}S$; c – SO_4^{2-} monodentate; d – SO_4^{2-} bidentate

two endothermic steps (50–98°C, $t_{max\ DTG}$=78 and 81°C, and 155–181°C, $t_{max\ DTG}$=164°C) corresponding to the evolving of a one half of water molecules each (calcd./found: 7.04/7.53% and 7.04/6.49%). The IR spectra (Fig. 9) support this affirmation due to the disappearance with increasing temperature of the strong and wide band from 3550–3200 cm^{-1} and weak one from 1200–950 cm^{-1} assigned to the OH stretching vibrations of water. Except these vibrations, no infrared activity was detected in the FTIR spectrum (Fig. 9a), which is characteristic for sulfides.

The next two processes (181–260 and 260–311°C) represent the formation of copper sulfide with lower content of sulfur, namely $Cu_{1.8}S$ and Cu_2S (calcd./found: 11.74/11.88% and 1.57/1.56%). The oxidation of evolved sulfur is responsible for the registered exothermic effect. Like the unreacted CuS, no infrared active phases were detected in FTIR spectrum (Fig. 9b).

The formed Cu_2S is instable, a gradual exothermic mass gain occurring in the temperature range

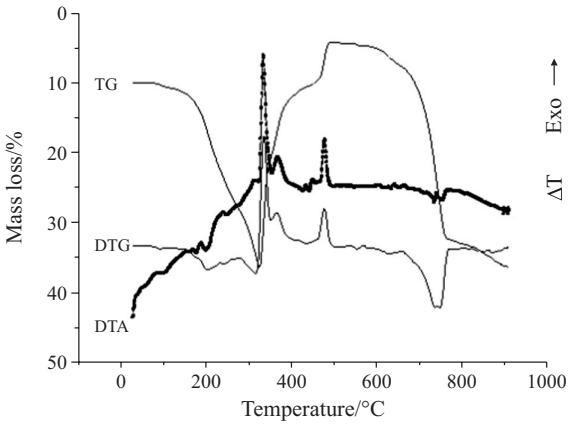

Fig. 10 TG, DTG and DTA curves of $CuS{\cdot}0.7H_2O$ obtained from Cu^{2+}:$S_2O_3^{2-}$ (1:6) system

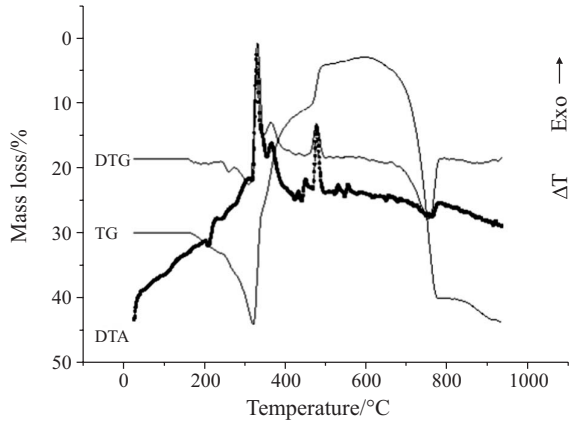

Fig. 11 TG, DTG and DTA curves of CuS obtained from Cu^{2+}:$S_2O_3^{2-}$ (1:4) system

(311–435°C, $t_{max\ DTG}$=325 and 335°C), assigned to $Cu^{+}\rightarrow Cu^{2+}$ and $S^{2-}\rightarrow SO_4^{2-}$ oxidation and $CuO\cdot CuSO_4$ formation (calcd./found: 35.21/34.80%). The FTIR spectra registered for the intermediates isolated in this temperature range Figs 9c and d evidenced a change of SO_4^{2-} group binding mode from mono- to bidentate one with temperature increase [40].

The oxysulfates stable in a large temperature range (435–652°C) decompose via three endothermic steps on further heating (652–855°C) to CuO (calcd./found: 35.21/34.82%).

The thermal behaviour of $CuS\cdot H_2O$ obtained from Cu^{2+}:V^{5+}:$S_2O_3^{2-}$ (1:1:6) system may be expressed by the following reactions.

$$CuS\cdot H_2O\rightarrow CuS\cdot 0.5H_2O+0.5H_2O$$

$$CuS\cdot 0.5H_2O\rightarrow CuS+0.5H_2O$$

$$1.8CuS+0.8O_2\rightarrow Cu_{1.8}S+0.8SO_2$$

$$2Cu_{1.8}S+0.2O_2\rightarrow 1.8Cu_2S+0.2SO_2$$

$$Cu_2S+2.5O_2\rightarrow CuO\cdot CuSO_4$$

$$CuO\cdot CuSO_4\rightarrow 2CuO+SO_2+0.5O_2$$

Copper sulfide $CuS\cdot 0.7H_2O$ obtained from Cu^{2+}:SO_4^{2-} (1:6) system evolved adsorbed water (calcd./found: 11.72/12.01%) in the temperature range 77–160°C ($t_{max\ DTG}$=92°C).

The anhydrous CuS release further sulfur (160–322°C) leading to Cu_2S formation (calcd./found: 14.79/14.27%). The decomposition stage is a complex one, three peaks were identified on DTG curve (199, 245 and 314°C). Unlike the first investigated case, it was not possible to discriminate the formation as reaction intermediate of $Cu_{1.8}S$.

The formed unstable sulfide, is oxidized in the temperature range 322–486°C. The DTG curve registered four peaks (334, 363, 418 and 447°C), comparative with two identified in the first sample. The mass gain of 32.07% corresponds to the formation of 0.87 moles of $CuO\cdot CuSO_4$ and 0.13 moles of CuO. The final temperature of the oxidation is ~50°C higher comparative with the first sulfide.

The final decomposition stage, representing the sulfate decomposition with CuO formation (calcd./found: 32.07/32.20%), occurs through two processes (586–774 and 777–908°C). The initial temperature of sulfate oxidation is ~130°C lower comparative with the first case.

In the following reactions is presented the thermal behaviour of $CuS\cdot 0.7H_2O$ obtained from Cu^{2+}:$S_2O_3^{2-}$ (1:6) system:

$$CuS\cdot 0.7H_2O\rightarrow CuS+0.7H_2O$$

$$2CuS+O_2\rightarrow Cu_2S+SO_2$$

$$0.94Cu_2S+2.3O_2\rightarrow 0.87CuO\cdot CuSO_4+0.13CuO+0.06SO_2$$

$$CuO\cdot CuSO_4\rightarrow 2CuO+SO_2+0.5O_2$$

The third investigated copper sulfide obtained from Cu^{2+}:$S_2O_3^{2-}$ (1:4) system is converted into $Cu_{1.8}S$ (calcd./found: 13.59/14.01%) in the temperature range 161–322°C. As in the second case three peaks are detected on DTG curve (195, 261 and 308°C).

The oxidation of $Cu_{1.8}S$ to $CuO\cdot CuSO_4$ (calcd./found: 40.09/40.66%) takes place in the temperature range 322–585°C, being associated with three (332, 366 and 477°C)/ five (330, 366, 432, 449, 480°C) peaks on DTG/DTA curves.

The oxysulfates decompose to CuO (calcd./found: 40.09/40.77%) through two steps (608–783 and 814–934°C).

The following reactions present the assumed thermal behaviour of CuS.

$$1.8CuS+0.8O_2\rightarrow Cu_{1.8}S+0.8SO_2$$

$$2Cu_{1.8}S+4.7O_2\rightarrow 1.8CuO\cdot CuSO_4+0.2SO_2$$

$$CuO\cdot CuSO_4\rightarrow 2CuO+SO_2+0.5O_2$$

Conclusions

The oxidation of copper sulfide (CuS) is complex in nature. The associated solid state transformations depend upon history of the sulfides.

The ammonium metavanadate has an important influence in the morphology of CuS particles. Thus the presence of vanadium in the system induce a densification of CuS nodules, but do not change the hexagonal CuS structure.

Depending on the starting CuS, changes of both thermal induced reactions stoichiometries and their temperature range occurrence are evidenced. Thus, although the formation of lower sulfur content sulfides, occurs practically in the same temperature range

(~160–~320°C), for the first two investigated samples a conversion $CuS \rightarrow Cu_2S$ is evidenced, while the sulfur elimination from the copper sulfide CuS obtained from Cu^{2+}:$S_2O_3^{2-}$ (1:4) system conducts only to $Cu_{1.8}S$. The further oxidation of sulfides, lead to $CuO \cdot CuSO_4$ for CuS obtained from Cu^{2+}:V^{5+}:$S_2O_3^{2-}$ (1:1:6) and Cu^{2+}:$S_2O_3^{2-}$ (1:6) systems, and to an oxysulfate with excess of CuO for Cu^{2+}:$S_2O_3^{2-}$ (1:6) system. The stability of the oxysulfates obtained is different: 23°C for Cu^{2+}:$S_2O_3^{2-}$ (1:4) system, 100°C for Cu^{2+}:$S_2O_3^{2-}$ (1:6) system and 217°C for Cu^{2+}:V^{5+}:$S_2O_3^{2-}$ (1:1:6) system. The particle dimensions have an important role in the thermal stability and the stoichiometry of the thermal decompositions. Thermal decomposition of lower CuS particles can be used to obtain Cu_2S, and bigger particle CuS can be used to $Cu_{1.8}S$ obtained.

The stability of oxysulfates depends on CuS particle dimensions. It was observed that the oxysulfates obtained from CuS with greater particle dimensions stability is 23°C, and for CuS with lower particle dimensions oxysulfates stability is 100°C.

Acknowledgements

The authors (Claudia Maria Simonescu, Valentin Serban Teodorescu, Oana Carp, Luminita Patron, Camelia Capatina) acknowledge the Ministry of Education and Research (Romania) for financial support (CEEX Program No. 6113/12.10.2005 'Methods and mechanisms for crystalline nanoparticles with shape and dimensions controlled for applications in bionanotechnology, sensors, plating and catalysis synthesis').

References

1 S. M. Stuczynski, Y. U. Kow and M. L. Steigerwald, J. Organomet. Chem., 167 (1993) 449.
2 M. T. S. Nair and P. K. Nair, Semicond. Sci. Technol., 4 (1989) 191.
3 P. C. Rieke and S. B. Bentjen, Chem. Mater., 5 (1993) 43.
4 T. Yamamoto, Y. Tanaka, E. Kubota and K. Osakada, Chem. Mater., 5 (1993) 1352.
5 I. Grozdanov and M. Najdoski, J. Solid State Chem., 114 (1995) 469.
6 D. C. Reynolds, G. Leies, L. T. Antes and R. E. Marburger, Phys. Rev., 96 (1954) 533.
7 K. W. Boer, Phys. Status Solidi A, 40 (1977) 435.
8 M. T. S. Nair, G. Alvarrez-Garcia, C. A. Estrada-Gasva and P. K. Nair, J. Electrochem. Soc., 140 (1993) 212.
9 P. K. Nair, M. T. Nair, A. Fernandez and M. Ocampo, J. Phys. D., 22 (1989) 829.
10 P. K. Nair, V. M. Garcia, A. M. Fernandez, H. S. Ruiz and M. T. S. Nair, J. Phys. D., 24 (1991) 441.
11 Z. H. Han, Y. P. Li, H. Q. Zhao, S. H. Yu, Y. L. Yin and Y. T. Qian, Mater. Lett., 44 (2000) 366.
12 W. Smykatz-Kloss, J. Thermal. Anal., 23 (1982) 15.
13 W. Smykatz-Kloss and K. Hausmann, J. Thermal Anal., 39 (1993) 1209.
14 J. G. Dunn and C. Muzenda, Thermochim. Acta, 369 (2001) 117.
15 R. Blachnik and A. Müller, Termochim. Acta, 361 (2000) 31.
16 R. Blachnik and A. Müller, Thermochim. Acta, 366 (2001) 47.
17 B. F. Ali, W. S. Al-Akramawi, K. H. Al-Obaidi and A. H. Al-Karboli, Thermochim. Acta, 419 (2004) 39.
18 L. Gao, E. Wang, S. Suoyuan, Z. Kang, Y. Lan and D. Wu, Solid State Commun., 130 (2004) 309.
19 J. R. Botelho, A. G. Souza, A. D. Gondim, P. F. Athayde-Filho, P. O. Dunstan, C. D. Pinheiro, E. Longo and L. H. Carvalho, J. Therm. Anal. Cal., 79 (2005) 309.
20 J. C. D'Ars de Figueiredo Jr., V. M. De Bellis, M. I. Yoshida, V. F. Cunha Lins and L. A. Cruz Souza, J. Therm. Anal. Cal., 79 (2005) 313.
21 S. P. Chen, X. X. Mung, O. Shuai, B. J. Jiao, S. L. Gao and Q. Z. Shi, J. Therm. Anal. Cal., 86 (2006) 767.
22 A. Kontny, H. De Wall, T. G. Sharp and M. Pósfai, Am. Mineral., 85 (2000) 1416.
23 E. Godočiková, P. Baláž, J. M. Criado, C. Real and E. Gock, Thermochim. Acta, 440 (2006) 19.
24 S. A. A. Jayaweera, J. H. Moss and A. Wearmouth, Thermochim. Acta, 152 (1989) 237.
25 I. D. Shah and S. E. Khalafalla, Metall. Trans., 2 (1971) 605.
26 C. Maurell, Bull. Soc. Française de Minéralogie et Cristallographie, 87 (1964) 377.
27 E. M. Bollin, Chalcogenides, in R. C. Mackemzie (Ed.), Differential Thermal Analysis, Academic Press, London 1970, p. 202.
28 R. I. Razouk, G. A. Kolta and R. S. Mikhail, J. Appl. Chem., 12 (1962) 190.
29 I. D. Shah and S. E. Khalafalla, Metall. Trans., 1 (1970) 2151.
30 J. G. Dunn and C. Muzenda, J. Therm. Anal. Cal., 64 (2001) 1241.
31 Ž. Živković, N. Štrabac, D. Živković, V. Velonski and I. Mihajlović, J. Therm. Anal. Cal., 79 (2005) 715.
32 L. Patron, O. Carp, I. Mindru, M. Pascu, N. Stanica, V. Ciupina, E. Segal and M. Brezeanu, J. Therm. Anal. Cal., 72 (2003) 271.
33 J. P. Sanders and P. K. Gallagher, J. Therm. Anal. Cal., 72 (2003) 777.
34 I. Mihajlović, J. Therm. Anal. Cal., 79 (2005) 715.
35 H. J. Gotsis, A. C. Barnes and P. Strange, J. Phys.: Condens. Matter, 4 (1992) 10461.
36 Y. Takeuchi, Y. Kudoch and G. Sato, Z. Kristallogr., 173 (1985) 119.
37 C. M. Simonescu, L. Patron, V. S. Teodorescu, M. Brezeanu and C. Capatina, J. Optoelectr. Adv. Mater., 8 (2006) 597.
38 C. M. Simonescu, V. S. Teodorescu, M. Brezeanu and A. Melinescu, Rev. Chim., 56 (2005) 611.
39 H. P. Klug and L. E. Alexander, in X-Ray Diffraction Procedures, Wiley, New York 1954, p. 461.
40 K. Nakamoto, in Infrared and Raman spectra of Inorganic and Coordination Compounds, Ed. 4., J. Wiley 1986, p. 252.

DOI: 10.1007/s10973-006-8079-z